Contribution from the Departments of Chemistry, Texas A&M University, College Station, Texas 77843, and Princeton University, Princeton, New Jersey 08540

The Tungsten–Tungsten Triple Bond. 5. Chlorine Atom Substitution Reactions Involving Dichlorotetrakis(diethylamido)ditungsten. Preparation, Properties, Structures, and Dynamical Solution Behavior of Bis(trimethylsilylmethyl)-, Dibromo-, and Diiodotetrakis(diethylamido)ditungsten

MALCOLM H. CHISHOLM,*[1a] F. ALBERT COTTON,*[1b] MICHAEL W. EXTINE,[1a] MICHELLE MILLAR,[1b] and B. RAY STULTS*[1b]

Received July 26, 1976 AIC60544J

$W_2Br_2(NEt_2)_4$ was obtained as an unexpected product in the reaction between $W_2Cl_2(NEt_2)_4$ and MeLi (1 equiv) due to the fortuitous presence of LiBr in commercially available ethereal solutions of the latter. $W_2Cl_2(NEt_2)_4$ reacts smoothly with LiBr (>2 equiv) and HgI_2 (>2 equiv) in diethyl ether to give $W_2Br_2(NEt_2)_4$ and $W_2I_2(NEt_2)_4$, respectively. *anti*-$W_2Cl_2(NEt_2)_4$ reacts with $LiCH_2SiMe_3$ (2 equiv) in benzene to give *anti*-$W_2(CH_2SiMe_3)_2(NEt_2)_4$ which, under thermodynamic control, isomerizes to a mixture of anti and gauche rotamers: a $\rightleftarrows$ g, $K = 4$. A bimolecular four-center mechanism in which alkyl-for-chlorine atom exchange occurs with retention of configuration at tungsten and without cleavage of the tungsten-to-tungsten bond is proposed. Activation parameters for the anti to gauche isomerization of $W_2(CH_2SiMe_3)_2(NEt_2)_4$ have been determined from ^1H NMR studies at 20, 54, 61, and 76 °C: $\Delta G^{\ddagger} = 24.2 \pm 1.0$ kcal mol^{-1} and $\Delta S^{\ddagger} = 2.4 \pm 3.4$ eu. Variable-temperature ^1H and ^{13}C NMR studies show that the compounds $W_2X_2(NEt_2)_4$, where X = Br and I, exist as anti rotamers in toluene-d_8. The free energy of activation for proximal–distal ethyl exchange is the same, within experimental error, for both compounds: $\Delta G^{\ddagger} = 15.4 \pm 0.4$ kcal mol^{-1}. The two compounds are isomorphous, crystallizing in space group $P\bar{1}$ with $Z = 2$. Unit cell dimensions and some important bond lengths for $W_2Br_2(NEt_2)_4$ are as follows: $a = 9.754$ (1) Å, $b = 15.724$ (3) Å, $c = 8.647$ (2) Å, $\alpha = 97.10$ (2)°, $\beta = 104.96$ (2)°, $\gamma = 86.64$ (1)°, $V = 1271.0$ (4) Å^3, W–W = 2.301 (2) Å, W–Br = 2.481 (6) Å, W–N = 1.90 (2) Å. Unit cell dimensions and some important bond lengths for $W_2I_2(NEt_2)_4$ are as follows: $a = 9.773$ (2) Å, $b = 15.983$ (5) Å, $c = 8.907$ (2) Å, $\alpha = 97.37$ (2)°, $\beta = 106.33$ (2)°, $\gamma = 86.42$ (2), $V = 1326.6$ (6) Å^3, W–W = 2.300 (4) Å, W–I = 2.682 (2) Å, W–N = 1.94 (3) Å. The molecules are centrosymmetric, with an anti rotational conformation.

Introduction

Several molecules containing triple bonds between tungsten atoms have recently been described and structurally characterized. These include $W_2(NMe_2)_6$,[2] $W_2(NEt_2)_6$,[2] $W_2Cl_2(NEt_2)_4$,[3] $W_2(NMe_2)_2(NEt_2)_4$,[3] $W_2Me_2(NEt_2)_4$,[3,4] $W_2(CH_2SiMe_3)_6$,[5,6] $W_2Me_2(O_2CNEt_2)_4$[7] and $W_2(O_2CNMe_2)_6$.[7] The dialkylamido compounds $W_2(NR_2)_6$ and $W_2X_2(NEt_2)_4$, where R = Me or Et and X = Cl or Me, show particularly interesting dynamical solution behavior. They are molecular propellers[8] and are stereochemically correspondent to the aryl-substituted ethanes Ar_3C-CAr_3 and XAr_2C-CAr_2X.[9] Rotations about W–N bonds may interchange proximal and distal ethyl groups rapidly on the NMR time scale without effecting rotation about the W–W bond. However, rotation about the W–W bond may occur and has been observed for $W_2Me_2(NEt_2)_4$. In order to obtain a detailed understanding of the dynamical solution behavior of the molecules of this type, it is necessary to reduce the symmetry of the system and thereby generate more permutationally distinguishable modes. A molecule seemingly well suited for such investigations was $Me(NEt_2)_2W{\equiv}W(NEt_2)_2Cl$; each tungsten atom is effectively labeled and anti–gauche isomerization is expected. We thus hoped to synthesize $W_2(Cl)(Me)(NEt_2)_4$ and to establish both the threshold mechanism for proximal–distal ethyl group exchange and the threshold mechanism for anti–gauche isomerization.

In this paper, we describe our attempts to synthesize and isolate $W_2(Me)(Cl)(NEt_2)_4$ and the related compound $W_2Cl(CH_2SiMe_3)(NEt_2)_4$. Our attempts failed, but our efforts did yield some interesting and unexpected findings. We report herein that the reaction between *anti*-$W_2Cl_2(NEt_2)_4$ and $LiCH_2SiMe_3$ (2 equiv) is stereospecific in giving *anti*-$W_2(CH_2SiMe_3)_2(NEt_2)_4$ which then isomerizes to the equilibrium mixture of anti and gauche rotamers. The preparation, some chemical properties, crystal structures, and dynamical solution behavior of two additional members of the $W_2X_2(NEt_2)_4$ series are also reported, namely, those with X = Br and X = I.

Results and Discussion

Synthesis. The red crystalline compound $W_2Cl_2(NEt_2)_4$ and MeLi (2 equiv) reacted to give the red crystalline compound $W_2Me_2(NEt_2)_4$.[6] $W_2Cl_2(NEt_2)_4$ and MeLi (1 equiv) reacted in ether to give, upon crystallization from hexane, red crystals of similar appearance and solubility to $W_2X_2(NEt_2)_4$ where X = Cl and Me. The ^1H NMR spectrum of these red crystals was complex and led us to believe that $W_2(Cl)(Me)(NEt_2)_4$ or a mixture of species might be present. A portion of the crystals was set aside for x-ray studies.

In the mass spectrum a number of W_2-containing ions were seen, including some ions of unexpectedly high mass and unusual isotopic distribution. The parent ion is shown in Figure 1 and has a mass greater than that of the sum of the reactants: $W_2Cl_2(NEt_2)_4$ + MeLi. The *m/e* distribution of this ion could not be accommodated for any $W_2Cl_2Li_y$ combination. However, when the red crystals were reacted with further MeLi, $W_2Me_2(NEt_2)_4$ was obtained. Thus we were led to believe that the crystals contained intermediates in the synthesis of $W_2Me_2(NEt_2)_4$ from $W_2Cl_2(NEt_2)_4$ and MeLi.

X-ray studies of the red crystals obtained from the reaction between $W_2Cl_2(NEt_2)_4$ and MeLi were thwarted by a number of problems (see x-ray section). It seemed that some of the crystals could be formulated as *anti*-$W_2(Me)_{1.5}(X)_{0.5}(NEt_2)_4$, where X was Br rather than Cl. At this point, we reexamined the mass spectra of this and related samples and found that the ion shown in Figure 1 corresponded to $W_2Br_2(NEt_2)_4^+$. Similarly we identified $W_2(Me)(Br)(NEt_2)_4^+$ in the mass spectrum.

The only conceivable explanation for these findings seemed to be that our commercial source of MeLi (Alfa) was contaminated with LiBr (which is soluble in diethyl ether and is formed in the preparation of MeLi from MeBr and Li metal) and that the exchange reaction W–Cl + LiBr → W–Br + LiCl had occurred.

We then reacted $W_2(NEt_2)_4Cl_2$ with LiBr (>2 equiv) in

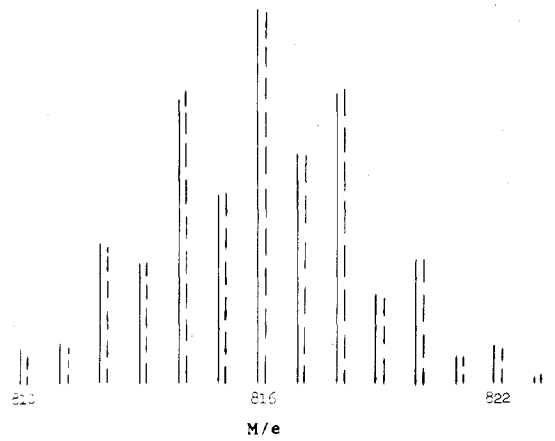

Figure 1. Observed (—) vs. computed (- - -) m/e distribution for the $W_2Br_2(NEt_2)_4^+$ ion found in the mass spectrometer at 100 °C, 70 eV.

diethyl ether and obtained, upon cooling a hexane extraction of this mixture, the red crystalline solid $W_2Br_2(NEt_2)_4$. A similar reaction involving $W_2Cl_2(NEt_2)_4$ and HgI_2 in ether gave $W_2I_2(NEt_2)_4$ as a red crystalline solid.

We reconsidered our initial objective, namely the preparation of $W_2(Me)(Cl)(NEt_2)_4$. Even using methyllithium free of LiBr, it seemed that we would be unlikely to obtain this compound in a pure state and in large quantities (ca. 1 g) owing to the very similar physical properties of crystalline samples of $W_2(Me)_x(Cl)_y(NEt_2)_4$ where $x + y = 2$ and $x = 0 \rightarrow 2$. Consequently we turned our attention to syntheses involving the more bulky trimethylsilylmethyl ligand (R = CH_2SiMe_3) hoping that steric factors would (i) slow down the second chlorine-for-alkyl exchange reaction [$W_2Cl_2(NEt_2)_4$ + LiR → $W_2(Cl)(R)(NEt_2)_4(k_1)$; $W_2(Cl)(R)(NEt_2)_4$ + LiR → $W_2R_2(NEt_2)_4$ k_2; $k_1 > k_2$] and (ii) cause the crystalline properties of the compounds $W_2Cl_xR_{2-x}(NEt_2)_4$, where x = 0–2, to be significantly different from each other.

$W_2Cl_2(NEt_2)_4$ reacted smoothly with $LiCH_2SiMe_3$ (2 equiv) in benzene or hexane solutions to give $W_2(CH_2SiMe_3)_2(NEt_2)_4$ which has been isolated as a red crystalline compound. However, attempts to prepare $W_2Cl(CH_2SiMe_3)(NEt_2)_4$ yielded only mixtures of $W_2Cl_2(NEt_2)_4$ and $W_2(CH_2SiMe_3)_2(NEt_2)_4$ which were separated by careful crystallization taking advantage of the higher solubility of the alkyl derivative. Even when the reaction was carried out in an NMR tube and monitored by NMR spectroscopy (see later), we failed to detect the compound $W_2Cl(CH_2SiMe_3)(NEt_2)_4$. Thus it appears that the second chlorine atom for alkyl group exchange reaction occurs faster than the first. Alkyl ligands are well known to exert a high trans influence in square-planar and octahedral complexes.[10] They also exert a high trans effect and thereby enhance the rate of substitution in the trans position. It is quite conceivable that a similar phenomenon could exist in the dinuclear compounds under consideration: the initial substitution of CH_2SiMe_3 for Cl could activate the remaining anti W–Cl bond toward substitution, the effect being transmitted via the W–W bond.

Physical Properties. The compounds $W_2X_2(NEt_2)_4$, where X = Br, I, and CH_2SiMe_3, are red crystalline compounds and are soluble in hydrocarbon solvents such as benzene and hexane. They are moisture sensitive but appear to be indefinitely stable when stored in vacuo or in sealed vials under an atmosphere of dry nitrogen. They are thermally quite stable and may be sublimed at ca. 120 °C (10^{-4} cmHg). In the mass spectrum they show molecular ions $W_2X_2(NEt_2)_4^+$ together with many other W_2-containing ions.

Infrared Spectra. A number of compounds of the general formula $W_2X_2(NEt_2)_4$ have now been prepared and characterized. In the crystalline state all adopt the anti rotameric form. Infrared data in the range 200–600 cm^{-1} are recorded in the Experimental Section. In this region we expect to observe W–N and W–X stretching modes, although, as we have shown previously,[2] these may not be pure modes. For $W_2X_2(NEt_2)_4$, where X = Cl, Br, I, Me, and CH_2SiMe_3, strong bands at 530 ± 10 and 585 ± 5 cm^{-1} may be associated with ν_{str}(W–N). For X = Me and CH_2SiMe_3, strong bands at 495 and 462 cm^{-1} respectively may be associated with ν_{str}(W–C). For X = Cl and Br strong bands at 350 and 220 cm^{-1}, respectively, probably correspond to ν_{str}(W–X).

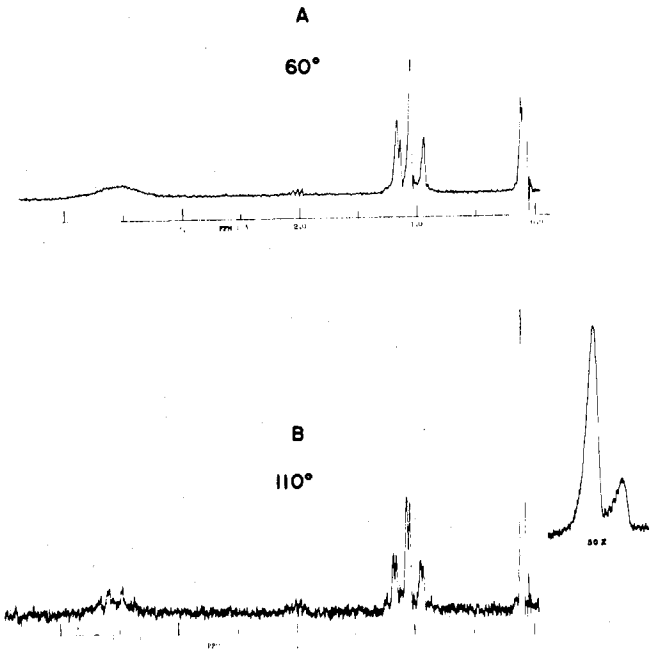

Figure 2. ^1H NMR spectra of $W_2(CH_2SiMe_3)_2(NEt_2)_4$ recorded in toluene-d_8 at 60 MHz: A, spectrum of a-I rapidly heated to +60 °C; B, $t = \infty$ spectrum at +110 °C where [g-I]/[a-I] = ca. 5; the $CH_2Si\mathit{Me}_3$ resonances are shown at scale expansion ×50.

^1H NMR Studies. The variable-temperature ^1H NMR spectra of $W_2X_2(NEt_2)_4$ where X = Br or I in toluene-d_8 were very similar to those previously described for $W_2Cl_2(NEt_2)_4$. They suggested the presence of only the anti rotamer in solution; this was confirmed by ^{13}C NMR studies (see later). The ^1H NMR spectra of $W_2(CH_2SiMe_3)_2(NEt_2)_4$ were more complicated and warrant specific comment.

$W_2(CH_2SiMe_3)_2(NEt_2)_4$, freshly prepared and dissolved in toluene-d_8 at ca. 35 °C, showed a single resonance at δ 0.08 ppm (relative to TMS) assignable to the $CH_2Si\mathit{Me}_3$ protons. With time a new resonance at δ 0.12 ppm (relative to TMS) grew at the expense of the former. This we attribute to the isomerization reaction

$$\textit{anti}\text{-}W_2(CH_2SiMe_3)_2(NEt_2)_4 \rightleftarrows \textit{gauche}\text{-}W_2(CH_2SiMe_3)_2(NEt_2)_4 \quad K \simeq 4\ (25\ ^\circ C) \qquad (1)$$

The assignment of anti and gauche rotamers is possible from a consideration of the ^1H NMR spectra. For example, when crystals of $W_2(CH_2SiMe_3)_2(NEt_2)_4$ were dissolved in toluene-d_8 and rapidly heated to +60 °C in the probe of an A-60 ^1H NMR spectrometer, the spectrum shown in Figure 2A was observed. At this temperature the rate of proximal–distal alkyl exchange was sufficiently fast to make the $N(CH_2\mathit{CH}_3)_2$ protons equivalent thus producing a well-resolved 1:2:1 triplet, J_{HH} = 7 Hz. The methylene protons of the trimethylsilylmethyl ligand also appeared as a singlet in this region. Only in the anti rotamer are all eight diethylamido ethyl groups equivalenced by the combined operations of the symmetry

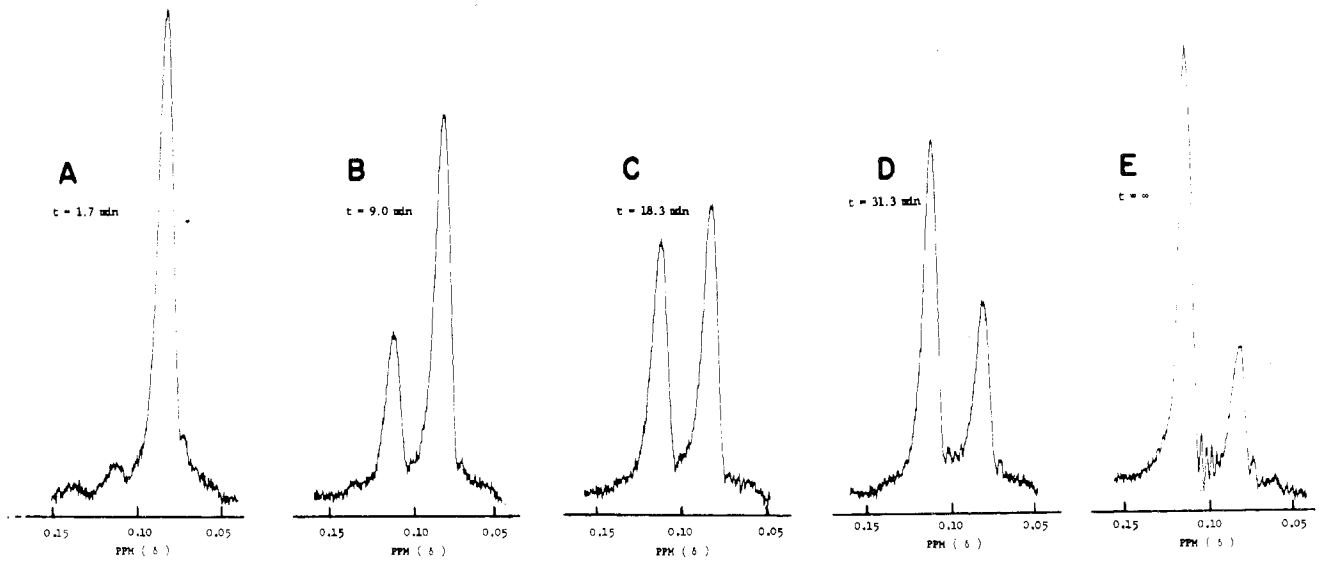

Figure 3. ^{1}H NMR spectra of the CH_2SiMe_3 resonances recorded at 54 °C during the anti to gauche isomerization reaction of $W_2(CH_2SiMe_3)_2(NEt_2)_4$: A, t = 1.7 min; B, t = 9 min; C, t = 18.3 min; D, t = 31.3 min; E, $t = \infty$.

group C_{2h}, to which the $W_2Cl_2N_4$ moiety belongs, and W–N bond rotations. Under the above conditions, rapid heating of a freshly dissolved sample to +60 °C, the concentration of the gauche rotamer, [g], was small relative to that of the anti rotamer, [a]. With time, the spectrum became more complex and then relatively simple when [g] > [a]. The t_∞ spectrum, recorded at 110 °C, is shown in Figure 2B. The $N(CH_2CH_3)_2$ resonance appeared as two sets of overlapping 1:2:1 triplets. This was expected for the gauche rotamer since there are two independent pairs of NEt_2 ligands: the $W_2C_2N_4$ moiety belongs to the symmetry group C_2. This assignment was also confirmed by ^{13}C NMR studies: at +80 °C the $N(CH_2CH_3)_2$ carbons appear as three resonances of relative intensity ca. 2:2:1. This situation parallels that previously described for $W_2Me_2(NEt_2)_4$: even at high temperatures (100 °C) anti $\rightleftarrows$ gauche isomerization is slow on the NMR time scale.

We have monitored the anti to gauche isomerization of $W_2(CH_2SiMe_3)_2(NEt_2)_4$ by ^{1}H NMR spectroscopy making the assumption that [a] and [g] can be determined by the measurement of the peak heights of the CH_2SiMe_3 proton resonances. These resonances appear as sharp singlets in a region of the spectrum well separated from other signals. See Figure 3. For the anti $\rightarrow$ gauche reaction of $W_2(CH_2SiMe_3)_2(NEt_2)_4$ we calculate $\Delta G^\ddagger = 24.2 \pm 1.0$ kcal mol^{-1} and $\Delta S^\ddagger = 2.4 \pm 3.4$ eu. $\Delta G^\ddagger$ for anti to gauche isomerization in $W_2(CH_2SiMe_3)_2(NEt_2)_4$ is ca. 3 kcal mol^{-1} higher than that previously determined[4] for $W_2Me_2(NEt_2)_4$. It is not unreasonable to suppose that this, at least in part, reflects the greater steric demand of the CH_2SiMe_3 ligand relative to the methyl ligand. However, the mechanism of anti–gauche isomerization remains unknown.

The stereochemistry of the substitution reaction leading to $W_2(CH_2SiMe_3)_2(NEt_2)_4$ has been investigated as follows. $W_2Cl_2(NEt_2)_4$ and $LiCH_2SiMe_3$ (2.2 equiv) were dissolved in toluene-d_8 in an NMR tube. The reaction was then followed by ^{1}H NMR spectroscopy at 40 °C. See Figure 4. Within ca. 22 min the formation of $W_2(CH_2SiMe_3)_2(NEt_2)_4$ was complete and the [a] to [g] ratio was ca. 4:1. The equilibrium concentration of rotamers, [a]/[g] = ca $^1/_4$, was attained within ca. 48 h at 40 °C. Significantly, during the course of the reaction no CH_2SiMe_3 resonance due to an intermediate, e.g., $W_2(Cl)(CH_2SiMe_3)(NEt_2)_4$, was detected although it could be that such a resonance was obscured by one of the resonances due to *anti*- or *gauche*-$W_2(CH_2SiMe_3)_2(NEt_2)_4$ or -$LiCH_2SiMe_3$. Even if this were the case, the lifetime of the intermediate would have to be short since the reaction was complete within ca. 22 min.

^{13}C NMR Studies. A variable-temperature carbon-13 NMR study was undertaken for the compounds $W_2X_2(NEt_2)_4$, where X = Br, I, and CH_2SiMe_3. The spectra obtained for the trimethylsilylmethyl compound parallel those previously reported[4] for $W_2Me_2(NEt_2)_4$ and are consequently not discussed further. Spectra recorded at various temperatures in toluene for the compounds X = Br and I are shown in Figures 5 and 6 respectively.

At the low-temperature limit (–25 °C) both $W_2Br_2(NEt_2)_4$ (Figure 5) and $W_2I_2(NEt_2)_4$ (Figure 6) exhibit only two sets of carbon-13 peaks which are assigned to the proximal and distal ethyl substituents of the anti rotamer. There is no observable quantity of the gauche rotamer present. In this respect, these compounds are completely analogous to their chloro analogue[11] but are different from the methyl analogue. The bromo or iodo compounds may each be heated at 100 °C and then cooled to –25 °C whereupon the original –25 °C spectra are recovered, without the slightest change. It seems likely that the gauche isomers are thermodynamically if not also kinetically inaccessible under these conditions. Temperature-dependent changes do occur between –25 and +100 °C all of which can be attributed to rotation about the W–NEt_2 bond resulting in the rapid interchange and consequent magnetic equivalence of the proximal and distal ethyl groups. The rotation process is illustrated most dramatically for the set of methylene carbon peaks which are separated by large chemical shift differences at –25 °C, viz., for $W_2Br_2(NEt_2)_4$, $\Delta\delta$ = 22.63 ppm, and for $W_2I_2(NEt_2)_4$, $\Delta\delta$ = 24.94 ppm. As the samples are warmed, the peaks broaden, disappear (T = 51 °C), coalesce (T = 70 ± 5 °C), and reemerge as a single but broad resonance (T = 110 °C) centered at δ 49.85 ppm (X = Br) and δ 50.50 ppm (X = I). Concomitant spectral changes are observed for peaks assigned to the methyl carbons which at –25 °C are located at δ 14.46 and 14.23 ppm, $\Delta\delta$ = 0.23 ppm for $W_2Br_2(NEt_2)_4$, and at δ 14.76 and 14.27 ppm, $\Delta\delta$ = 0.49 ppm for $W_2I_2(NEt_2)_4$. At 9 °C, the methyl peaks have merged into a single peak centered at δ 14.43 ppm (X = Br) and δ 14.27 ppm (X = I) and continue to sharpen as the temperature is increased. Activation parameters estimated for the proximal–distal exchange (methylene carbons) of both the bromo and iodo derivative are identical within experimental error, viz., $\Delta G^\ddagger = 15.3 \pm 0.4$ kcal/mol.

Solid-State Structures: $W_2X_2(NEt_2)_4$; X = Br, I. Each

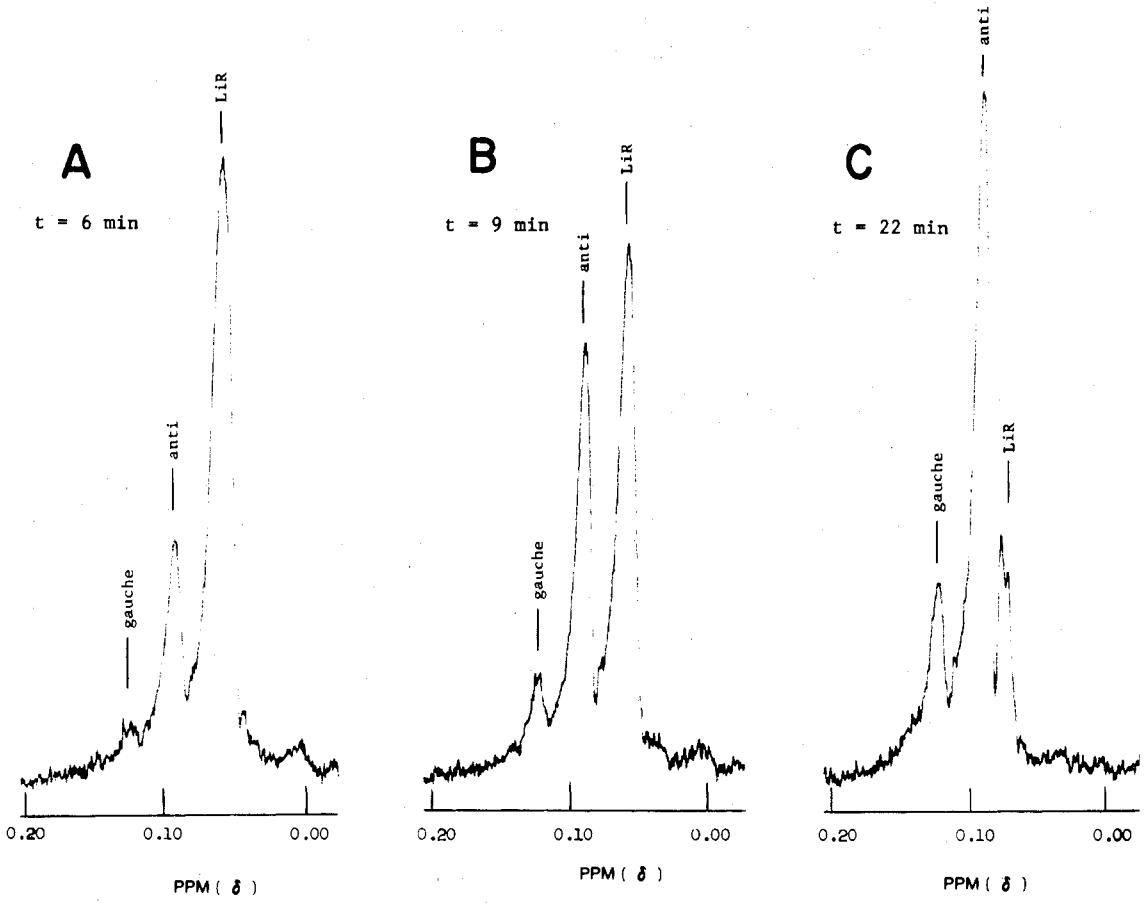

Figure 4. ^{1}H NMR spectra showing the CH_2SiMe_3 resonances recorded at various times during the reaction between *anti*-$W_2Cl_2(NEt_2)_4$ and $LiCH_2SiMe_3$ (2.2 equiv) at 40 °C: A, t = 6 min; B, t = 9 min; C, t = 22 min.

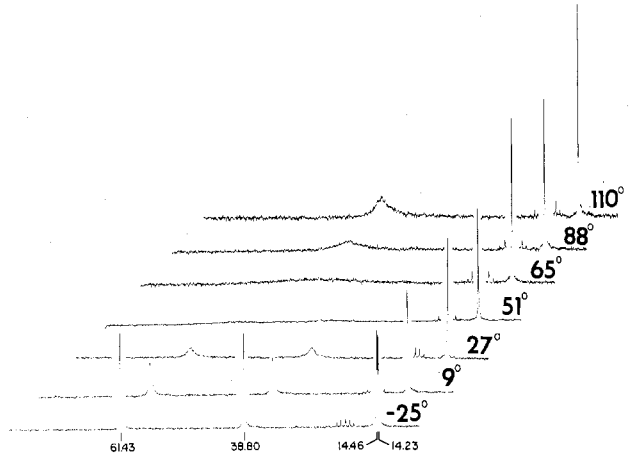

Figure 5. ^{13}C NMR spectra of $W_2Br_2(NEt_2)_4$ as a function of temperature. Chemical shifts are downfield from TMS in ppm.

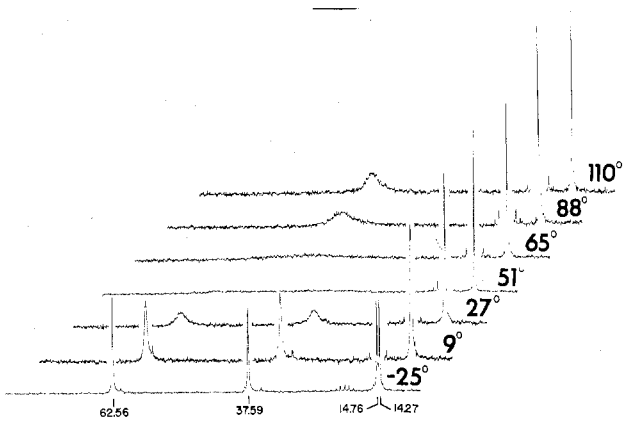

Figure 6. ^{13}C NMR spectra of $W_2I_2(NEt_2)_4$ as a function of temperature. Chemical shifts are downfield from TMS in ppm.

compound is composed of discrete molecules, of either $W_2Br_2[N(C_5H_5)_2]_4$ or $W_2I_2[N(C_2H_5)_2]_4$, in the solid state. The two compounds are isomorphous; i.e., the molecules pack in essentially the same way, in space group $P\bar{1}$. The two molecules in each unit cell are crystallographically independent, but each one has rigorous C_i ($\bar{1}$) symmetry since the midpoint of each of the W≡W bonds lies on one of the crystallographic centers of inversion at 0, 0, 0 and $^1/_2$, $^1/_2$, 0. The crystallographic asymmetric unit is thus composed of two half-molecules. A perspective drawing showing the coordination geometry about the tungsten atoms in $W_2Br_2(NEt_2)_4$ and the atom-labeling scheme used for both molecule I and molecule II is presented in Figure 7. Since both molecule I and molecule II are essentially identical, only molecule I is shown, but the labeling scheme for molecule II is also shown on this figure. Likewise, a view of molecule I and the atom-labeling scheme for both molecules in $W_2I_2(NEt_2)_4$ are given in Figure 8. Final atomic coordinates and final thermal parameters for $W_2Br_2(NEt_2)_4$ and $W_2I_2(NEt_2)_4$ are given in Tables I and II, respectively.

The bond distances and bond angles for $W_2Br_2(NEt_2)_4$ and $W_2I_2(NEt_2)_4$ are given in Tables III and IV, respectively. The equations for some mean planes and the dihedral angles for the bromo and iodo compounds are listed in Tables V and VI, respectively. No nonbonded intermolecular contacts significantly less than the sum of the van der Waals radii for the corresponding atoms were observed.

It is interesting to note that in the series $W_2X_2(NEt_2)_4$, with X = Cl, Br, I, and Me, all of the crystalline compounds contain

Table I. Atomic Positional and Thermal Parameters[a,b] for $W_2Br_2(NEt_2)_4$

Atom	x	y	z	β_{11}	β_{22}	β_{33}	β_{12}	β_{13}	β_{23}
W(1)	0.122 19 (9)	−0.000 90 (6)	0.0315 (1)	0.005 43 (9)	0.002 66 (4)	0.0096 (1)	−0.0018 (1)	0.0050 (2)	−0.0005 (1)
W(2)	0.516 90 (9)	0.511 70 (6)	0.1374 (1)	0.006 20 (1)	0.002 91 (4)	0.0058 (1)	−0.0017 (1)	0.0006 (2)	0.0000 (1)
Br(1)	0.210 9 (3)	−0.086 1 (2)	0.2615 (3)	0.011 9 (3)	0.004 8 (1)	0.0138 (4)	−0.0002 (3)	0.0044 (6)	0.0033 (4)
Br(2)	0.407 3 (3)	0.393 0 (2)	0.2245 (3)	0.013 4 (3)	0.004 6 (1)	0.0123 (4)	−0.0047 (3)	0.0075 (5)	0.0032 (3)
N(1)	0.165 (2)	−0.050 (1)	−0.166 (2)	0.007 (2)	0.003 5 (9)	0.009 (3)	0.001 (2)	0.001 (4)	−0.001 (3)
N(2)	0.163 (2)	0.118 (1)	0.087 (2)	0.008 (2)	0.003 8 (9)	0.012 (3)	−0.000 (2)	0.012 (4)	0.002 (3)
N(3)	0.419 (2)	0.618 (1)	0.159 (2)	0.008 (2)	0.005 5 (10)	0.010 (3)	−0.006 (2)	−0.004 (4)	0.008 (3)
N(4)	0.716 (2)	0.514 (1)	0.216 (2)	0.002 (2)	0.004 7 (10)	0.019 (4)	0.000 (2)	−0.005 (5)	0.003 (3)
C(1)	0.315 (2)	−0.040 (2)	−0.170 (3)	0.006 (2)	0.005 5 (13)	0.013 (4)	−0.003 (3)	0.008 (5)	−0.002 (4)
C(2)	0.338 (3)	0.032 (2)	−0.266 (4)	0.011 (3)	0.008 5 (18)	0.020 (5)	−0.008 (4)	0.005 (7)	0.003 (5)
C(3)	0.074 (3)	−0.084 (2)	−0.329 (3)	0.010 (3)	0.004 4 (12)	0.012 (4)	−0.003 (3)	−0.003 (6)	−0.007 (4)
C(4)	0.122 (4)	−0.178 (2)	−0.381 (4)	0.022 (5)	0.006 0 (16)	0.023 (5)	−0.005 (5)	0.021 (8)	−0.011 (5)
C(5)	0.074 (3)	0.200 (1)	0.068 (3)	0.011 (3)	0.001 7 (9)	0.017 (4)	−0.000 (3)	0.007 (6)	−0.000 (3)
C(6)	0.090 (3)	0.239 (2)	−0.086 (4)	0.016 (4)	0.005 0 (13)	0.027 (5)	−0.002 (4)	0.011 (7)	0.012 (4)
C(7)	0.322 (2)	0.135 (2)	0.162 (3)	0.005 (3)	0.005 4 (13)	0.014 (4)	−0.005 (3)	0.001 (5)	−0.002 (4)
C(8)	0.356 (3)	0.159 (2)	0.342 (3)	0.011 (3)	0.008 3 (17)	0.016 (5)	−0.009 (4)	0.004 (7)	−0.008 (5)
C(9)	0.360 (3)	0.686 (1)	0.068 (3)	0.012 (3)	0.003 0 (10)	0.018 (4)	−0.000 (3)	0.012 (6)	0.006 (3)
C(10)	0.464 (3)	0.762 (2)	0.095 (4)	0.020 (4)	0.003 1 (11)	0.030 (6)	−0.002 (4)	0.017 (8)	0.007 (4)
C(11)	0.415 (3)	0.648 (2)	0.338 (3)	0.015 (4)	0.005 7 (14)	0.008 (3)	0.002 (4)	0.007 (6)	−0.000 (4)
C(12)	0.268 (3)	0.645 (2)	0.363 (4)	0.020 (4)	0.008 1 (19)	0.027 (5)	0.006 (5)	0.032 (7)	0.001 (6)
C(13)	0.772 (3)	0.547 (2)	0.391 (3)	0.010 (3)	0.005 0 (12)	0.007 (3)	−0.004 (3)	−0.002 (5)	0.001 (3)
C(14)	0.824 (3)	0.638 (2)	0.423 (4)	0.019 (5)	0.006 6 (16)	0.017 (5)	−0.011 (4)	0.004 (8)	−0.010 (5)
C(15)	0.836 (2)	0.509 (2)	0.128 (3)	0.008 (3)	0.005 0 (12)	0.015 (4)	−0.001 (3)	0.009 (5)	0.006 (4)
C(16)	0.952 (3)	0.441 (2)	0.191 (3)	0.009 (3)	0.008 5 (19)	0.015 (4)	0.002 (4)	0.010 (6)	0.001 (5)

[a] Figures in parentheses are the estimated standard deviations in the least significant figures. [b] The form of the anisotropic thermal parameter is $\exp[-(\beta_{11}h^2 + \beta_{22}k^2 + \beta_{33}l^2 + \beta_{12}hk + \beta_{13}hl + \beta_{23}kl)]$.

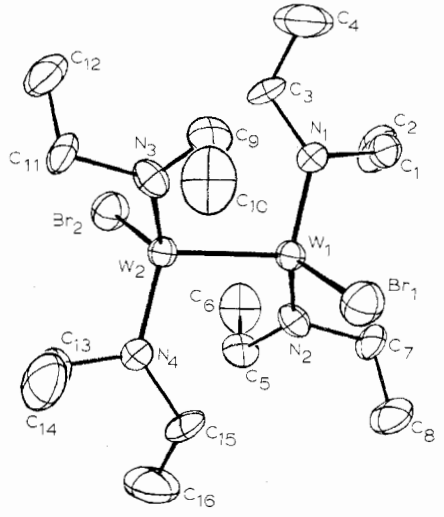

Figure 7. ORTEP perspective view of molecule I in the unit cell of $W_2Br_2(NEt_2)_4$. The conformation of molecule II is virtually indistinguishable. The labels on the right are for molecule I, while those on the left pertain to molecule II; each molecule has a center of symmetry; the other atom of each pair related by the center is designated with a primed label.

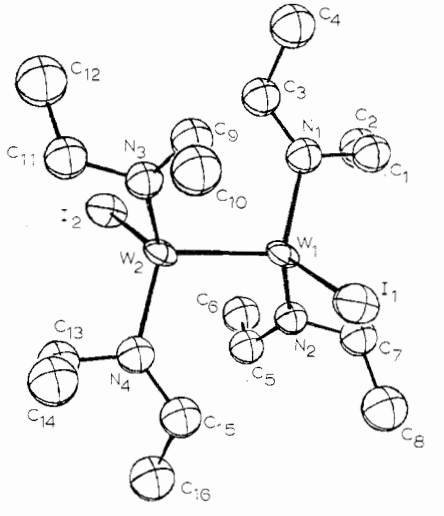

Figure 8. ORTEP perspective drawing of molecule I of $W_2I_2(NEt_2)_4$. The conformation of molecule II is virtually indistinguishable. The labels on the right are for molecule I, while those on the left pertain to molecule II; each molecule has a center of symmetry; the other atom of each pair related by the center is designated with a primed label.

exclusively the anti rotamers, but the intermolecular packing is variable. There are three different crystal structures, one for X = Cl ($P2_1/n$), one for X = Me ($C2/c$), and one for X = Br, I ($P\bar{1}$).

A comparison of the six known structures of compounds containing a triple bond between tungsten atoms reveals a high degree of consistency in bond lengths (Table VII). All compounds having four or six NR_2 groups have a W≡W bond length of 2.291 (1)–2.301 (2) Å, whereas in $W_2(CH_2SiMe_3)_6$ the distance is 0.04 Å shorter. It has already been suggested that this may be due to the fact that N→W π bonding may be slightly competitive with W–W π bonding. In the entire set of NR_2-containing compounds, the W–N distances are substantially invariant (the range 1.91–1.97 Å is not significant in view of the esd's) with an average value 1.94 ± 0.03 Å that is, as noted previously,[4] about 0.10 Å shorter than might be expected for a W–N (sp^2) single bond if the W–X distances are used to estimate a single-bond radius for W in these systems. This too can be explained by invoking N→W π bonding.[12] The values of the W single-bond radius, listed in the column headed $d_{W-X} - d_{X-X}$ are essentially constant, with an average value of 1.36 ± 0.04 Å.

Mechanism of Halide Substitution Reactions. Our observation that the *anti*-$W_2Cl_2(NEt_2)_4$ reacts with $LiCH_2SiMe_3$ (2 equiv) stereospecifically to give *anti*-$W_2(CH_2SiMe_3)_2(NEt_2)_4$ which under thermodynamic control isomerizes to the gauche rotamer allows for some interesting speculation concerning the mechanism of substitution. If we make the assumption that substitution occurs in a stepwise process involving the intermediate $W_2(Cl)(CH_2SiMe_3)(NEt_2)_4$, then substitution of CH_2SiMe_3 for Cl must occur with retention of configuration at tungsten. If the exchange reaction proceeded with inversion at tungsten or was accompanied by W–W bond rotation, then the gauche product would be ki-

Table II. Atomic Positional and Thermal Parameters[a,b] for $W_2I_2(NEt_2)_4$

Atom	x	y	z	β_{11}	β_{22}	β_{33}	β_{12}	β_{13}	β_{23}
W(1)	0.1222 (2)	0.000 46 (7)	0.0314 (2)	0.0090 (2)	0.002 07 (5)	0.0087 (2)	0.0034 (1)	0.0067 (3)	0.0007 (1)
W(2)	0.5203 (2)	0.515 69 (7)	0.1342 (1)	0.0091 (2)	0.002 16 (5)	0.0052 (1)	0.0040 (1)	0.0028 (3)	0.0015 (1)
I(1)	0.2227 (3)	−0.087 3 (1)	0.2789 (3)	0.0163 (4)	0.003 66 (9)	0.0117 (3)	0.0059 (3)	0.0064 (6)	0.0046 (3)
I(2)	0.4065 (3)	0.394 4 (1)	0.2392 (3)	0.0167 (4)	0.003 49 (9)	0.0112 (3)	0.0023 (3)	0.0093 (6)	0.0047 (3)

Atom	x	y	z	B, Å^2	Atom	x	y	z	B, Å^2
N(1)	0.166 (3)	−0.051 (2)	−0.167 (3)	3.6 (6)	C(7)	0.312 (4)	0.133 (2)	0.160 (5)	4.2 (8)
N(2)	0.166 (3)	0.117 (2)	0.089 (3)	3.2 (6)	C(8)	0.362 (6)	0.167 (3)	0.332 (6)	6.3 (11)
N(3)	0.421 (3)	0.622 (1)	0.167 (3)	2.1 (5)	C(9)	0.352 (4)	0.683 (2)	0.033 (5)	4.3 (8)
N(4)	0.726 (3)	0.521 (2)	0.204 (3)	3.6 (6)	C(10)	0.458 (6)	0.757 (3)	0.054 (6)	6.3 (11)
C(1)	0.313 (4)	−0.037 (2)	−0.160 (5)	4.2 (8)	C(11)	0.414 (4)	0.651 (2)	0.318 (4)	3.8 (7)
C(2)	0.321 (5)	0.033 (3)	−0.270 (5)	5.4 (10)	C(12)	0.275 (5)	0.649 (3)	0.345 (5)	5.3 (10)
C(3)	0.078 (4)	−0.084 (2)	−0.312 (5)	4.2 (8)	C(13)	0.775 (5)	0.550 (2)	0.386 (5)	4.9 (9)
C(4)	0.123 (5)	−0.176 (3)	−0.371 (5)	5.4 (10)	C(14)	0.829 (6)	0.638 (3)	0.412 (6)	6.4 (11)
C(5)	0.089 (4)	0.196 (2)	0.070 (4)	3.9 (8)	C(15)	0.834 (5)	0.511 (3)	0.135 (5)	5.4 (10)
C(6)	0.092 (5)	0.241 (3)	−0.067 (5)	4.9 (9)	C(16)	0.968 (5)	0.451 (3)	0.204 (5)	5.7 (10)

[a] Figures in parentheses are the estimated standard deviations in the least significant figures. [b] The form of the anisotropic thermal parameters is $\exp[-(\beta_{11}h^2 + \beta_{22}k^2 + \beta_{33}l^2 + \beta_{12}hk + \beta_{13}hl + \beta_{23}kl)]$.

Table III. Bond Distances and Bond Angles[a] within $W_2Br_2(NEt_2)_4$

Bond Distances, Å			
W(1)-W(1)′	2.303 (2)	W(2)-W(2)′	2.299 (2)
W(1)-Br(1)	2.476 (3)	W(2)-Br(2)	2.488 (3)
W(1)-N(1)	1.92 (2)	W(2)-N(3)	1.89 (2)
-N(2)	1.92 (2)	-N(4)	1.89 (2)
N(1)-C(1)	1.49 (3)	N(3)-C(9)	1.42 (3)
-C(3)	1.51 (3)	-C(11)	1.57 (3)
N(2)-C(5)	1.50 (3)	N(4)-C(13)	1.51 (3)
-C(7)	1.54 (3)	-C(15)	1.54 (3)
C(1)-C(2)	1.54 (4)	C(9)-C(10)	1.57 (4)
C(3)-C(4)	1.57 (4)	C(11)-C(12)	1.51 (4)
C(5)-C(6)	1.58 (4)	C(13)-C(14)	1.52 (4)
C(7)-C(8)	1.51 (3)	C(15)-C(16)	1.54 (4)
Bond Angles, Deg			
W(1)′-W(1)-Br(1)	107.82 (8)	W(2)′-W(2)-Br(2)	108.30 (8)
W(1)′-W(1)-N(1)	103.4 (5)	W(2)′-W(2)-N(3)	101.1 (5)
-N(2)	102.2 (5)	-N(4)	103.5 (6)
Br(1)-W(1)-N(1)	115.0 (5)	Br(2)-W(2)-N(3)	112.8 (6)
-N(2)	112.9 (6)	-N(4)	113.9 (6)
N(1)-W(1)-N(2)	114.0 (8)	N(3)-W(2)-N(4)	115.7 (8)
W(1)-N(1)-C(1)	114 (1)	W(2)-N(3)-C(9)	139 (1)
-C(3)	133 (1)	-C(11)	113 (1)
-N(2)-C(5)	134 (1)	-N(4)-C(13)	116 (2)
-C(7)	113 (1)	-C(15)	132 (2)
C(1)-N(1)-C(3)	112 (2)	C(9)-N(3)-C(11)	107 (2)
C(5)-N(2)-C(7)	113 (2)	C(13)-N(4)-C(15)	110 (2)
N(1)-C(1)-C(2)	115 (2)	N(3)-C(9)-C(10)	99 (2)
-C(3)-C(4)	111 (2)	-C(11)-C(12)	112 (2)
N(2)-C(5)-C(6)	109 (2)	N(4)-C(13)-C(14)	115 (2)
-C(7)-C(8)	113 (2)	-C(15)-C(16)	112 (2)

[a] Figures in parentheses are the estimated standard deviations in the least significant figures.

Table IV. Bond Distances and Bond Angles[a] within $W_2I_2(NEt_2)_4$

Bond Distances, Å			
W(1)-W(1)′	2.296 (2)	W(2)-W(2)′	2.304 (2)
W(1)-I(1)	2.682 (2)	W(2)-I(2)	2.681 (2)
W(1)-N(1)	2.00 (2)	W(2)-N(3)	1.93 (2)
-N(2)	1.91 (1)	-N(4)	1.93 (2)
N(1)-C(1)	1.45 (3)	N(3)-C(9)	1.61 (3)
-C(3)	1.39 (3)	-C(11)	1.39 (3)
N(2)-C(5)	1.43 (3)	N(4)-C(13)	1.56 (3)
-C(7)	1.42 (4)	-C(15)	1.36 (4)
C(1)-C(2)	1.60 (4)	C(9)-C(10)	1.59 (4)
C(3)-C(4)	1.58 (4)	C(11)-C(12)	1.44 (4)
C(5)-C(6)	1.50 (4)	C(13)-C(14)	1.50 (4)
C(7)-C(8)	1.51 (4)	C(15)-C(16)	1.60 (4)
Bond Angles, Deg			
W(1)′-W(1)-I(1)	107.1 (7)	W(2)′-W(2)-I(2)	108.1 (6)
W(1)′-W(1)-N(1)	103.5 (6)	W(2)′-W(2)-N(3)	106.4 (5)
-N(2)	104.1 (6)	-N(4)	101.9 (6)
I(1)-W(1)-N(1)	115.1 (6)	I(2)-W(2)-N(3)	109.3 (5)
-N(2)	110.9 (6)	-N(4)	115.6 (6)
N(1)-W(1)-N(2)	114.9 (8)	N(3)-W(2)-N(4)	114.8 (7)
W(1)-N(1)-C(1)	110 (2)	W(2)-N(3)-C(9)	125 (2)
-C(3)	132 (2)	-C(11)	119 (2)
-N(2)-C(5)	136 (2)	-N(4)-C(13)	110 (2)
-C(7)	115 (2)	-C(15)	136 (2)
C(1)-N(1)-C(3)	117 (2)	C(9)-N(3)-C(11)	116 (2)
C(5)-N(2)-C(7)	108 (2)	C(13)-N(4)-C(15)	114 (2)
N(1)-C(1)-C(2)	110 (2)	N(3)-C(9)-C(10)	108 (2)
-C(3)-C(4)	114 (2)	-C(11)-C(12)	115 (2)
N(2)-C(5)-C(6)	118 (2)	N(4)-C(13)-C(14)	109 (2)
-C(7)-C(8)	120 (2)	-C(15)-C(16)	119 (2)

[a] Figures in parentheses are the estimated standard deviations in the least significant figures.

netically accessible. It is very difficult to imagine that the reaction proceeds with cleavage of the tungsten–tungsten bond to give mononuclear tungsten intermediates which then react to generate the thermodynamically unfavored rotamer. The simplest and most logical mechanistic interpretation is that substitution of CH_2SiMe_3 for Cl occurs by a bimolecular four-center exchange mechanism schematically represented by I. The tungsten–tungsten bond is not cleaved, and, if the chlorine atom, the methylene carbon, and the two tungsten atoms are contained in the same plane, then the exchange of CH_2SiMe_3 for Cl will clearly proceed with retention of configuration at tungsten.

Substitution by a four-center mechanism is well documented in substitution reactions, particularly in alkyl-transfer reactions.[13] The alkoxides $M_2(OR)_6$, where M = Mo or W and R = CH_2CMe_3 or $SiMe_3$, are known to reversibly bind donor molecules such as amines to give dinuclear compounds $M_2(OR)_6L_2$.[14] Thus the proposal of a four-center exchange mechanism in which tungsten expands its coordination number

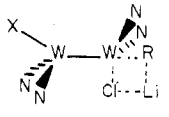

I

N = NEt_2
X = Cl or R
R = CH_2SiMe_3

Table V. Some Unit-Weighted Mean Planes in $W_2Br_2(NEt_2)_4$

Plane	Atoms in plane	Equation of plane[a] A	B	C	D
I	W(1)′-W(1)-Br(1)	0.1187	−0.7619	−0.6367	0.0001
II	W(1)′-W(1)-N(1)	0.1036	0.9531	−0.2845	0.0000
III	W(1)′-W(1)-N(2)	0.2300	0.1923	−0.9540	0.0001
IV	N(1)-C(1)-C(3)	−0.1057	0.9670	−0.2319	−0.4865
V	N(2)-C(5)-C(7)	0.3930	0.1186	−0.9118	0.1443
VI	W(2)′-W(2)-Br(2)	−0.8316	0.5420	−0.1215	−0.1852
VII	W(2)′-W(2)-N(3)	−0.8764	−0.4752	−0.0780	−8.4079
VIII	W(2)′-W(2)-N(4)	0.5430	0.7843	−0.3000	9.4246
IX	N(3)-C(9)-C(11)	−0.9154	−0.3616	−0.1770	−7.6218
X	N(4)-C(13)-C(15)	−0.1122	0.9698	−0.2166	6.4614

Planes	Dihedral angle, deg	Planes	Dihedral angle, deg
I-II	122.2	VI-VII	118.7
I-III	119.2	VI-VIII	121.2
II-III	118.6	VII-VIII	120.1
II-IV	12.4	VII-IX	8.9
III-V	10.5	VIII-X	13.1

[a] The equation of the plane is of the form $Ax + By + Cz - D = 0$.

Table VI. Some Unit-Weighted Mean Planes in $W_2I_2(NEt_2)_4$

Plane	Atoms in plane	Equation of plane[a] A	B	C	D
I	W(1)′-W(1)-I(1)	0.1323	−0.7721	−0.6215	0.0003
II	W(1)′-W(1)-N(1)	0.0926	0.9478	−0.3050	−0.0002
III	W(1)′-W(1)-N(2)	0.2313	0.2058	−0.9509	0.0001
IV	N(1)-C(1)-C(3)	−0.1313	0.9608	−0.2444	−0.5396
V	N(2)-C(5)-C(7)	0.4165	0.0878	−0.9049	0.1059
VI	W(2)′-W(2)-I(2)	−0.8239	0.5552	−0.1138	0.0272
VII	W(2)′-W(2)-N(3)	−0.8685	−0.4957	−0.0082	−8.5924
VIII	W(2)′-W(2)-N(4)	0.0279	0.9945	−0.1009	8.0810
IX	N(3)-C(9)-C(11)	−0.8910	−0.4139	−0.1865	−8.1454
X	N(4)-C(13)-C(15)	−0.0160	0.9831	−0.1822	7.5365

Planes	Dihedral angle, deg	Planes	Dihedral angle, deg
I-II	122.0	VI-VII	116.2
I-III	117.6	VI-VIII	122.7
II-III	120.4	VII-VIII	121.1
II-IV	13.3	VII-IX	11.3
III-V	12.9	VIII-X	5.3

[a] The equation of the plane is of the form $Ax + By + Cz - D = 0$.

Table VII. Comparison of Selected Bond Lengths, Å, in W≡W Compounds

Compd	$d_{W\equiv W}$	d_{W-N}	d_{W-X}	$d_{W-X} - d_{X-X}$
$W_2(NMe_2)_6$	2.293 (2)	1.97 (1)		
$W_2Me_2(NEt_2)_4$	2.291 (1)	1.97 (1)	2.171 (11)	1.40
$W_2Cl_2(NEt_2)_4$	2.301 (1)	1.94 (1)	2.332 (8)	1.35
$W_2Br_2(NEt_2)_4$	2.301 (2)	1.91 (2)	2.482 (3)	1.34
$W_2I_2(NEt_2)_4$	2.300 (2)	1.94 (4)	2.682 (2)	1.35
$W_2(CH_2SiMe_3)_6$	2.254 (2)		2.14 (4)	1.37

but retains the W–W bond has ample precedent.

The relative concentration of *gauche*-$W_2(CH_2SiMe_3)_2(NEt_2)_4$ formed at $t = 22$ min (see Figure 4), [g]/[a] ≃ 0.20, is ca. 10% larger than that expected from isomerization of the initially formed anti rotamer. A number of explanations could account for this observation. For example, the presence of significant[15] concentrations of *gauche*-$W_2Cl_2(NEt_2)_4$ in equilibrium with *anti*-$W_2Cl_2(NEt_2)_4$ or anti to gauche isomerization of an intermediate such as $W_2(Cl)(CH_2SiMe_3)(NEt_2)_4$ could contribute to the formation of *gauche*-$W_2(CH_2SiMe_3)_2(NEt_2)_4$.

We conclude that these observations provide further support for our proposal[2] concerning the formation of M_2L_6 compounds (M = Mo, W; L = CH_2SiMe_3, NR_2) from metathetic reactions involving molybdenum and tungsten halides ($MoCl_5$, $MoCl_3$, WCl_6, and WCl_4). We proposed that M_2L_6 compounds were formed from substitution reactions involving intermediates in which there already exists strong metal-to-metal bonding and not from the coupling of mononuclear ML_3 species or from homoleptic compounds such as $Mo(NR_2)_4$ or $W(NMe_2)_6$ which are also formed in those reactions. $W_2Cl_2(NEt_2)_4$ is prepared from the reaction between WCl_4 and $LiNEt_2$ and is labile to exchange reactions as in the formation of $W_2(NEt_2)_6$[3] and $W_2(CH_2SiMe_3)_2(NEt_2)_4$. The stereochemical course of the reaction leading to the latter compound suggests that cleavage of the tungsten to tungsten bond does not occur during the alkyl-for-chlorine exchange process.

Experimental Section

General procedures and the synthesis of $W_2Cl_2(NEt_2)_4$ have been described previously.[3]

NMR Measurements. Proton NMR spectra were recorded on a Varian A-60 spectrometer. The carbon-13 spectra were recorded on a Jeol PFT 100/Nicolet 1080 Fourier transform spectrometer operating at a frequency of 25.033 MHz. A sweep width of 4000 Hz at a tilt angle of 37° repeated at 1.2-s intervals was employed. The carbon-13 peak assigned to the unique substituted carbon of toluene-d_8 was used for the calibration and was taken to be 137.19 ppm downfield from TMS. The temperature was calibrated with a copper–constantan thermocouple inserted in a NMR tube placed in the spectrometer probe and connected to a Leeds and Northup Model 913 digital thermometer. At any dial setting of the variable-temperature unit, the temperature was constant to ±2 °C over the time required to record the spectrum.

Preparation of $W_2Br_2(NEt_2)_4$. LiBr (ca. 14 mmol) was prepared in situ from the reaction between LiBu (14.4 mmol) and $BrCH_2CH_2Br$ (35 mmol) in ether (20 ml). The solvent was removed, the LiBr was dried in vacuo, and then ether (120 ml) was added. $W_2(NEt_2)_4Cl_2$ (1.15 g, 1.58 mmol) was added to the LiBr slurry and the reaction mixture was stirred at 25 °C for 12 h. The solvent was stripped off, and the residue was dried in vacuo and then extracted with warm (50 °C) hexane (100 ml). The filtrate was concentrated to ca. 40 ml at 50 °C and then cooled slowly to −20 °C. The resulting red crystals were filtered off and dried; yield 0.96 g (74%, based on tungsten).

Anal. Calcd for $W_2(NEt_2)_4Br_2$: C, 23.67; H, 4.91; N, 6.88; Br, 19.69. Found: C, 23.55; H, 4.94; N, 6.87; Br, 19.59. Infrared data (600–200 cm^{-1}) (Nujol mull, CsI plates): 220 (s), 239 (m), 309 (m), 320 (w, sh), 502 (m), 530 (s), 583 (s), 596 (sh).

Preparation of $W_2(NEt_2)_4I_2$. HgI_2 (ca. 50 mmol) was prepared in situ from the reaction between I_2 and Hg, carried out in refluxing ether. The solution of HgI_2 (in ether, 50 ml) was added via syringe to a flask containing $W_2(NEt_2)_4Cl_2$ (1.54 g, 2.12 mmol). The solution was stirred for 3 h at 25 °C and then the solvent was stripped off. The residue was dried (30 min at 50 °C, 0.01 Torr) and then extracted with hexane (50 ml at 50 °C). The solvent was removed and the residue was purified via sublimation (120–140 °C, 10^{-3} Torr), followed by recrystallization from hexane; yield ca. 0.8 g of a dark red crystalline solid.

Anal. Calcd for $W_2(NEt_2)_4I_2$: C, 21.01; H, 4.32; N, 6.20; I, 28.03. Found: C, 21.12; H, 4.43; N, 6.16; I, 27.89. Infrared data (600–200 cm^{-1}) (Nujol mull, CsI plates): 233 (m), 303 (m), 315 (w, sh), 495 (m), 521 (s), 596 (s).

Preparation of $W_2(NEt_2)_4(CH_2SiMe_3)_2$. Me_3SiCH_2Li (340 mg, 260 mmol) in hexane (35 ml) was added to $W_2(NEt_2)_4Cl_2$ (1.27 g, 1.77 mmol) in hexane (40 ml), with stirring, at 50 °C. A white precipitate formed. After stirring of the mixture at 50 °C for 1 h, the solvent was stripped off and the residue was extracted with warm (50 °C) hexane (50 ml). The red solution was concentrated at 50 °C to ca. 20 ml and cooled slowly to −20 °C. The deep red crystals were filtered off and dried; yield ca. 0.3 g.

Anal. Calcd. for $W_2(NEt_2)_4(CH_2SiMe_3)_2$: C, 34.81; H, 7.35; N, 6.72. Found: C, 34.70; H, 7.52; N, 6.75. Infrared data (600–200 cm^{-1}) (Nujol mull, CsI plates): 278 (m), 300 (m), 313 (w), 462 (s), 487 (m), 518 (s), 584 (s), 596 (sh), 610 (sh).

Kinetics of the Anti → Gauche Isomerization of $W_2(NEt_2)_4(CH_2SiMe_3)_2$. Aliquots (0.5 ml each) of a stock solution of $W_2(NEt_2)_4(CH_2SiMe_3)_2$ (14 mg, 0.02 mmol per aliquot) in toluene-d_8 were sealed in NMR tubes and stored at −198 °C. Kinetic runs at

75.8, 61.1, and 54.2 °C, respectively, were carried out directly in the NMR probe. The estimated variation in the temperature is ±0.2 °C. The sample that was run at 20.0 °C was kept in a constant-temperature (20.0 ± 0.1 °C) bath and its NMR spectra were obtained in a cooled (20 °C) NMR probe. The relative concentrations of the anti and gauche isomers were determined by peak height measurements of the respective CH_2SiMe_3 methyl resonances. See Figure 3.

Raw Data. For T = 75.8 °C, time in s (% gauche): 110 (30), 155 (44), 195 (52), 235 (58), 285 (63), 320 (67), 390 (71), 435 (74), 515 (76). For T = 61.1 °C, time in s (% gauche): 90 (10), 310 (31), 420 (36), 725 (58), 975 (63), 1060 (63), 1105 (66), 1150 (67), 1250 (69). For T = 54.2 °C, time in s (% gauche): 100 (6), 155 (10), 230 (15), 340 (20), 455 (25), 540 (30), 625 (32), 685 (35), 805 (39), 930 (44), 1025 (47), 1100 (47), 1205 (51), 1340 (55), 1510 (58), 1720 (61), 1875 (64), 1930 (64), 2175 (67). For T = 20.0 °C, time in s (% gauche): 7380 (8.0), 24 600 (14.4), 74 580 (32.1), 114 900 (41.5), 163 800 (51.6), 210 000 (59.6), 292 500 (67.8).

Data Reduction. The anti to gauche isomerization was treated as opposing first-order reactions where k_1 and k_{-1} refer to the forward (anti → gauche) and reverse (gauche → anti) reactions, respectively. We define the quantities g_t and g_e as the percent gauche isomer at time t and at equilibrium, respectively; for these reactions g_e = 80%. A plot of $\ln [g_e/(g_e - g_t)]$ vs. time should yield a straight line of slope Ck_1 where $C = (100 - g_0)/g_e = 1.25$. The following rate constants were obtained (k, s^{-1} (T °C)): 4.97 (9) × 10^{-3} (75.8), 1.26 (5) × 10^{-3} (61.1), 6.74 (6) × 10^{-4} (54.2), 4.99 (7) × 10^{-6} (20.0). The free energies of activation, as calculated from Eyring's equation, are as follows ($\Delta G^{\ddagger}$, kcal mol^{-1} (T °C)): 24.2 (75.8), 24.1 (61.1), 24.0 (54.2), 24.3 (20.0). Other activation parameters, E_a = 25.5 ± 1.1 kcal mol^{-1}, $\Delta H^{\ddagger}_{298}$ = 24.9 ± 1.0 kcal mol^{-1}, and $\Delta S^{\ddagger}$ = 2 ± 3 eu, were calculated from an Arrhenius plot: $\log k = 31.7 - (12.84 \times 10^3)\ T^{-1}$.

Stereospecificity of the Reaction between $W_2(NEt_2)_4Cl_2$ and $LiCH_2SiMe_3$. $W_2(NEt_2)_4Cl_2$ (0.026 mmol) and $LiCH_2SiMe_3$ (0.07 mmol) were dissolved in toluene-d_8 (0.6 ml) and the solution was placed in an NMR tube. ^1H NMR spectra indicated that the substitution reaction was complete within ca. 22 min at 40 °C. See Figure 4. The anti-to-gauche ratio at t = 22 min was 4:1 and slowly decreased; the equilibrium ratio (anti:gauche = 1:4) was reached within 48 h.

X-Ray Crystallography for $W_2Br_2(NEt_2)_4$. Dark red crystals, suitable for data collection, were removed from a sealed container in a nitrogen-filled glovebag and immersed in heavy mineral oil which had been dried over sodium. An approximately equidimensional crystal, 0.242 × 0.238 × 0.266 mm, was sealed in a thin-walled glass capillary filled with mineral oil and used for data collection. Procedures used for crystal characterization and data collection have been previously described.[16] The crystal appeared to be of good quality, with ω scans for several intense reflections having peak widths at half-height ≤0.20°. Preliminary lattice constants and axial photographs indicated the symmetry crystal class to be no higher than triclinic. The unit cell volume corresponded to that expected for Z = 2; thus, the space group was assumed to be $P\bar{1}$. The choice of the centrosymmetric space group was supported at all stages of the subsequent structural solution and refinement.

Accurate lattice constants and the orientation matrix used to calculate setting angles during data collection were obtained from least-squares refinement of the diffraction geometry of 15 high-angle reflections, 20.0 ≤ 2θ(Mo Kα) < 35.0°, chosen to give a good sampling of Miller indices and setting angles. The lattice parameters are a = 9.754 (1) Å, b = 15.724 (3) Å, c = 8.647 (2) Å, α = 97.10 (2), β = 104.96 (2)°, γ = 86.64 (1)°, V = 1271.0 (4) Å^3.

Data were recorded using a Syntex $P\bar{1}$ autodiffractometer equipped with a graphite-crystal monochromator using Mo Kα radiation. Variable scan rates from 4.0 to 24.0°/min were used for symmetric θ–2θ scans from 1.0° below to 1.0 above the calculated Mo Kα_1–Mo Kα_2 doublet. The ratio of total background time to scan time was 0.50. A total of 3356 unique data having 0° < 2θ(Mo Kα) < 45.0° were recorded. Corrections for absorption effects[17] (μ = 129.21 cm^{-1}) were applied to all data. The minimum, maximum, and average transmission coefficients were 0.045, 0.185, and 0.100, respectively. Three standard reflections, measured every 150 reflections, showed no significant deviations and the data were reduced to a set of relative $|F_o|^2$ after corrections for Lorentz and polarization effects. Those 2157 data having $I > 3\sigma(I)$ were retained as observed and used in the final structure refinement.[18]

The atomic coordinates for the two unique tungsten atoms were derived from a three-dimensional Patterson synthesis. Contrary to the common situation in space group $P\bar{1}$ with Z = 2 in which the asymmetric unit consists of one complete molecule with an inversion center between the two molecules, this compound crystallizes so that the asymmetric unit consists of two half-molecules with the center of each intramolecular tungsten–tungsten vector occupying one of the crystallographic inversion centers at 0, 0, 0 and $^1/_2$, $^1/_2$, 0. The tungsten–tungsten vector for one molecule is nearly parallel to the a axis of the unit cell with the other vector lying along the c axis. The atomic coordinates for the two tungsten atoms were refined in two cycles of full-matrix least-squares refinement to give the discrepancy indices

$$R_1 = \Sigma ||F_o| - |F_c||/\Sigma |F_o| = 0.304$$

$$R_2 = [\Sigma w(|F_o| - |F_c|)^2/\Sigma w|F_o|^2]^{1/2} = 0.417$$

All least-squares refinements minimized the function $\sum w(|F_o| - |F_c|)^2$ where the weighting factor w is equal to $4|F_o|^2/\sigma^2(F_o^2)$ and σ is the esd of $|F_o|^2$. A value of 0.070 was used for p in the calculation[16] of $\sigma(F_o)^2$. The atomic scattering factors used in all least-squares refinements were those of Cromer and Waber.[19] Anomalous dispersion effects were included in the calculated scattering factors for tungsten and bromine.[20] The atomic coordinates for the remaining 22 nonhydrogen atoms of the asymmetric unit were then located from one difference Fourier map. The 24 atoms were refined employing anisotropic thermal parameters for the two tungsten atoms and isotropic thermal parameters for the remaining atoms to give R_1 = 0.077 and R_2 = 0.090. The structure was subsequently refined to convergence in four cycles of full-matrix least-squares refinement employing anisotropic thermal parameters for all atoms to give final residuals of R_1 = 0.051 and 0.065. During the final least-squares refinement no parameter shifted by more than 0.05σ, where σ is the estimated standard deviation of that parameter. A final difference Fourier map showed no features of structural significance. The highest peaks in the map were located between the tungsten atoms along the W≡W bonds. No attempt was made to locate the hydrogen atoms. An examination of the final observed and calculated structure factors showed no trends in reflection number, Miller indices, or $(\sin\theta)/\lambda$.

X-Ray Crystallography for $W_2I_2(NEt_2)_4$. Because of the similarity of the two compounds and the use of essentially identical procedures for both compounds, only deviations from the procedures used for $W_2Br_2(NEt_2)_4$ will be described. A crystal measuring 0.098 × 0.354 × 0.262 mm was sealed in a capillary filled with mineral oil. The compound was found to be isomorphous with the corresponding bromide compound. The lattice constants determined from the 15 reflections in the range 20.0° ≤ 2θ(Mo Kα) ≤ 35.0° are a = 9.773 (2) Å, b = 15.983 (5) Å, c = 8.907 (2) Å, α = 97.37 (2)°, β = 106.33 (2), γ = 86.42 (2)°, and V = 1326.6 (6) Å^3. In the range of 0° < 2θ(Mo Kα) < 45°, 3484 data recorded using variable scan rates from 4.0 to 24.0°/min were used for θ–2θ scans. Again, the scan range was from 2θ(Mo Kα_1) − 1.0° to 2θ(Mo Kα_2) + 1.0° with the ratio of background time to scan time equaling 0.50. The data were corrected for absorption effects (μ = 115.64 cm^{-1}) with the minimum, maximum, and average transmission coefficients being 0.023, 0.355, and 0.194, respectively. No effects of crystal decomposition were observed. The 2554 data having $I > 3\sigma(I)$ were used in the final structure refinement.

The final refined positional parameters from the corresponding bromide compound were used as initial parameters for $W_2I_2(NEt_2)_4$, with I atoms replacing Br atoms. The positional and isotropic thermal parameters for all 24 atoms were refined in three cycles of full-matrix least-squares refinement to give R_1 = 0.158 and R_2 = 0.186. The structural model was refined to convergence in four additional cycles of least-squares refinement employing anisotropic temperature parameters for the W and I atoms and isotropic temperature parameters for all remaining atoms to give final discrepancy values of R_1 = 0.092 and R_2 = 0.120. In view of the large absorption effects and the questionability of the crystal face measurements, resulting from the crystal being sealed under mineral oil, the structural refinement was terminated at this point. A final difference Fourier map, while indicating more spurious peaks than were observed for the bromo compound, revealed nothing of structural significance.

Tables of observed and calculated structure factors for the data used in the final refinements of each compound are available.[21]

Acknowledgment. We thank the Research Corp., the donors of the Petroleum Research Fund, administered by the American Chemical Society, and the National Science Foundation

(Grant No. MPS 73-05016) for support of this work at Princeton University and the National Science Foundation (Grant No. CHE 75-05509) for support at Texas A&M University.

Registry No. $W_2Br_2(NEt_2)_4$, 60803-45-4; $W_2(NEt_2)_4I_2$, 60803-46-5; $W_2(NEt_2)_4(CH_2SiMe_3)_2$, 60828-76-4; $W_2(NEt_2)_4Cl_2$, 57088-63-8; ^{13}C, 14762-74-4.

Supplementary Material Available: Listings of structure factor amplitudes (21 pages). Ordering information is given on any current masthead page.

References and Notes

(1) (a) Princeton University. (b) Texas A&M University.
(2) F. A. Cotton, B. R. Stults, J. M. Troup, M. H. Chisholm, and M. Extine, *J. Am. Chem. Soc.*, **97**, 1242 (1975); M. H. Chisholm, F. A. Cotton, M. Extine, and B. R. Stults, *ibid.*, **98**, 4477 (1976).
(3) M. H. Chisholm, F. A. Cotton, M. Extine, M. Millar, and B. R. Stults, *J. Am. Chem. Soc.*, **98**, 4486 (1976).
(4) M. H. Chisholm, F. A. Cotton, M. Extine, M. Millar, and B. R. Stults, *Inorg. Chem.*, **15**, 2244 (1976).
(5) W. Mowat, A. J. Shortland, G. Yagupsky, M. Yagupsky, N. J. Hill, and G. Wilkinson, *J. Chem. Soc., Dalton Trans.*, 533 (1972); F. Huq, W. Mowat, A. Shortland, A. C. Skapski, and G. Wilkinson, *Chem. Commun.*, 1079 (1971).
(6) M. H. Chisholm, F. A. Cotton, M. Extine, and B. R. Stults, *Inorg. Chem.*, **15**, 2252 (1976).
(7) M. H. Chisholm, F. A. Cotton, M. Extine, and B. R. Stults, *J. Am. Chem. Soc.*, **98**, 5683 (1976).
(8) K. Mislow, *Acc. Chem. Res.*, **9**, 26 (1976).
(9) P. Finocchiaro, W. D. Hounshell, and K. Mislow, *J. Am. Chem. Soc.*, **98**, 4952 (1976).
(10) T. G. Appleton, H. C. Clark, and L. E. Manzer, *Coord. Chem. Rev.*, **10**, 335 (1973).
(11) In a previous study[3] the presence of only *anti*-$W_2Cl_2(NEt_2)_4$ was deduced from variable-temperature ^1H NMR spectra and computer simulations.
(12) For a discussion of the significance of N to M π bonding in transition metal dialkylamides see D. C. Bradley and M. H. Chisholm, *Acc. Chem. Res.*, **9**, 273 (1976).
(13) F. Basolo and R. G. Pearson in "Mechanisms of Inorganic Reactions", Wiley, New York, N.Y., 1968, Chapter 3.
(14) M. H. Chisholm and M. W. Extine, *J. Am. Chem. Soc.*, **97**, 5625 (1975).
(15) If the a $\rightleftarrows$ g equilibrium favors *anti*-$W_2Cl_2(NEt_2)_4$, as was suggested previously,[3] but isomerization is rapid at 40 °C, and if the gauche rotamer were kinetically more labile to substitution than the anti rotamer, then "significant" concentrations of *gauche*-$W_2(CH_2SiMe_3)_2(NEt_2)_4$ would be formed initially.
(16) F. A. Cotton, B. A. Frenz, G. Deganello, and A. Shaver, *J. Organomet. Chem.*, **50**, 227 (1973).
(17) "International Tables for X-Ray Crystallography", Vol. III, Kynoch Press, Birmingham, England, 1965.
(18) The computer programs used for the structural solution and refinement were those of the Enraf-Nonius Structure Determination Package. The programs were used on a PDP 11/45 computer at the Molecular Structure Corp., College Station, Tex.
(19) D. T. Cromer and J. T. Waber, "International Tables for X-Ray Crystallography", Vol. IV, Kynoch Press, Birmingham, England, 1974, Table 2.3.1.
(20) D. T. Cromer and D. Liberman, *J. Chem. Phys.*, **53**, 1891 (1970).
(21) Supplementary material.

Contribution from the Department of Applied Chemistry, Faculty of Engineering, Osaka University, Yamadakami, Suita-Shi, Osaka-Fu, 565 Japan

Preparation and Properties of New Perovskite Type Oxides Containing Divalent Europium

KAZUNAO SATO,* HIROSHI KIYOKAWA, GIN-YA ADACHI,* and JIRO SHIOKAWA*

Received May 25, 1976 AIC603899

New mixed europium(II) oxides of the type $EuM_2M'O_{5.5}$ and $Eu_2MM'O_{5.5}$ (M = Ca, Sr, Ba; M' = Nb, Ta) were prepared by the reaction of europium sesquioxide, alkaline earth oxide, tantalum (or niobium) metal, and tantalum (or niobium) pentoxide at 1250–1350 °C under vacuum. The oxides obtained have an ordered cubic perovskite structure with oxygen deficiency. Divalent europium ions in the oxides occupy both 12-fold A sites and 6-fold B sites. The emission spectra of the divalent europium ions confirm the distribution of the divalent europium ions in these oxides.

Introduction

There are many perovskite type oxides of the divalent europium ion. McCarthy and Greedan[1] have proposed guidelines for the prediction of new perovskite type oxides $Eu(M,M')O_3$. One of them is a well-known Sr^{2+} analogue. An analogue of Sr_3WO_6, "Eu_3WO_6", is not a stable phase.[2] Brixner[3] reported the first defect perovskites $Ba_3TaO_{5.5}$ and $Sr_3TaO_{5.5}$. An analogue of $Sr_3TaO_{5.5}$, "$Eu_3TaO_{5.5}$", is not a stable phase as well as "Eu_3WO_6".[4] If the hypothetical oxide did exist, it would have the ordered perovskite $(NH_4)_3FeF_6$ structure type and one Eu^{2+} would have to occupy the 6-fold B sites. In previously known phases, Eu^{2+} occupies a site with a coordination number higher than 6 and this suggests that Eu^{2+} prefers a higher than 6-fold coordination number site in mixed oxides. Consequently, it seemed that Eu^{2+} would not be able to occupy the 6-fold B sites in the perovskite type oxides and would occupy only the 12-fold A sites.

In this study, we have discussed with the aid of crystal data and emission spectra whether Eu^{2+} would occupy the 6-fold B sites in some new prepared perovskite type oxides.

Experimental Section

Reagents. Europium sesquioxide was obtained from Shin-etsu Chemical Corp., in minimum purity of 99.9%. Niobium metal, niobium pentoxide, tantalum metal, tantalum pentoxide, and strontium oxide were purchased from Wako Chemical Industries, Ltd., in purity of 99.7%, 99.9%, 99.9%, 99.8%, and 99.0%, respectively. Calcium oxide (99.0%) and barium oxide (97.0%) were available from Kanto Chemical Corp. and Merck Corp., respectively. Alkaline earth oxides were calcined at 1200 °C for several hours under vacuum ($\sim 10^{-2}$ mmHg) before used in the preparation.

Preparation of $EuM_2M'O_{5.5}$. Starting mixtures were ground together in an agate mortar and pressed into pellets at 2400 kg/cm^2 and fired on a molybdenum plate at 1250–1350 °C under vacuum ($\sim 10^{-4}$ mmHg). Several conditions of starting mixture ratios and heating time were used in the preparation. The sample obtained from the starting mixture having the stoichiometric ratio always indicated lower Eu^{II} content than that expected regardless of heating time. The mixtures were heated for 24 h to improve homogenization, but the samples obtained also had lower Eu^{II} content. These phenomena are probably caused both by the volatilization of europium from Eu^{II} mixed oxides and by the effect of oxygen leakage into the furnace during the heating period.[5] Consequently, the most appropriate starting mixture ratio and heating time are Eu_2O_3:MO:M':M'_2O_5 = 1:4:0.6:0.7 (M=Ca, Sr, Ba; M' = Nb, Ta) and 3 h. The surface of each pellet heated was removed, and the residue was used as a sample for subsequent experiments.

Preparation of $Eu_2MM'O_{5.5}$. Starting mixtures (Eu_2O_3:MO:M':M'_2O_5 = 1:1:0.6:0.2) were treated as described in the preparation of $EuM_2M'O_{5.5}$.

Analytical Methods. The sample obtained was treated with hot concentrated hydrochloric acid. Europium ion dissolved as trivalent ion in the solution, and the alkaline earth ion also dissolved. The residue corresponded to M'_2O_5, from which the content of tantalum